ANALYSIS OF COOLING AIR JACKET AND AIR DISTRIBUTOR IN A CO-CURRENT SPRAY DRYER[*]

M. MOHAMMADI[1**], M. YAGHOUBI[2] AND E. GOSHTASBI RAD[2]

[1]Khouzestan Water & Power Authority, Ahwaz, I. R. of Iran
[2]Dept. of Mechanical Engineering, Shiraz University, Shiraz, I. R. of Iran
Email: moona_mohammadi@yahoo.com

Abstract– The purpose of the present study is to simulate a co-current pilot plant spray dryer with cooling air jacket, air distributor and pressure nozzle, using a numerical technique. For the spray dryer, cooled air enters its secondary wall which has a helical passage around the drum and the main process fluid enters in the axial flow direction from an air distributor which is located on the top center position of the dryer. Fluid flow and heat transfer from the inner fluid to the surrounding air jacket is studied with a special treatment to predict convection heat transfer through the helix. By knowing the air temperature and flow velocity entering the jacket and the thermal condition of the process fluid entering the drum in a counter-current direction, combined free and forced turbulent convection heat transfer in the drum are investigated using the RNG k-ε model of a turbulent model. Analyses were carried out using the SIMPLEC scheme and Euler-Lagrange model with and without spray water and milk to determine the pressure field, velocity distribution, temperature field of the process fluid throughout the drum and its wall, as well as the particles temperature and humidity, time of evaporation and diameter. Comparison of transient simulation of the particle size and time of evaporation with empirical relations is made for certain conditions. Validation of the numerical results with the experimental measurements shows good agreement.

Keywords– Cooling air jacket, spray dryer, free and forced convection, heat and mass transfer

1. INTRODUCTION

Spray drying is a process for converting a liquid feed into a powder by evaporation of the solvent. Compared to other evaporation process, spray drying has the great advantage that products can be dried without much loss of volatile or thermal labile compounds. These advantagecs are especially important in the production of food stuffs such as milk powder, instant coffee, etc. The product to be dried by this process can be categorized into two groups: non sticky and sticky products. Most process are relatively sticky, since some non sticky products will exhibit sticky behavior under certain conditions. The non sticky products can be dried using a simpler drier design. Sticky products are generally difficult to be spray died. During the drying process they may either remain as syrup or stick on the drier chamber wall. This can lead to lower product yields and some operating problems. To dry these materials successfully, the drier design has to be modified to some amount of additive that is added before drying. This method changes the product properties and increases the cost. Other methods are scraping the surface and using a very low temperature. These methods require specialized equipment to produce a desirable condition. One of the suitable ways to decrease sticking on the wall is to cool the chamber wall. By using cooling air jacket around the main chamber, the wall temperature and stickiness decreases [1-3]. Cooling air jacket is found to improve the process but not to resolve the problem completely. Several equipment models have been developed in the past decades. In most models, variations of air temperature and residence times are

neglected and the flow of air with solid particles is not considered. In a nutshell, with the CFD approach, the spray- air mixing is addressed by combining the airflow and particle trajectories, yielding temperature and humidity patterns in the drying chamber, which in turn, when combined with the particle trajectories, result in the air temperature and humidity histories of the particles. Some studies of the CFD approach are reported in literature. Oakley and Bahu [4] used FLOW3D to simulate the gas flow in a spray chamber. In this study a k-ε turbulence model is used. Zbicinski [5] suggested a model to calculate spray drying in a pilot plant dryer by using the computational fluid dynamics program to determine air flow theoretically. A drying model which described the relation between the process conditions of the drying process, energy consumption and the properties of the powder produced is studied by Strassma and Houlingen et.al [6]. In this study, by using the CFD technique and k-ε turbulent model, the gas flow in a spray dryer in two dimension is simulated and the trajectories and the course of drying process of the atomized particles is calculated. Kieviet [7] modelled and measured the air flow temperature and humidity patterns in a spray dryer. The modeling is based on a CFD package (CFX-F3D). Optimize process conditions for producing pomegranate juice powder with a spray dryer is done by Aziztaemeh, et al. [8]. The results show that malt dextrin with De=6 as a drying aid with a fruit juice to malt dextrin ratio equal to $\frac{65}{35}$ and %0.3 zinc stearate for the free flowing state give the best product. With a laboratory spray dryer the basic parameters for drying orange juice with a 65% concentration is studied by Chegini and Ghobadian [9]. According to this research the results of the statistical analysis of the experimental data show that the parameter of inlet air temperature and feed flow rate have a significant effect on the dryer yield and wall deposit of the spray dryer individually and jointly. Also, with the addition of liquid glucose the optimum conditions are obtained with a feed flow rate of 15 ml min, inlet air temperature of 130 ^{0}C and outlet air temperature of 85 ^{0}C. For the orange powder containing 2% moisture, the sticky point temperature was 44 ^{0}C. More recently the effect of spray penetration and evaporation has been studied by Khaleghi, et al. [10]. It is found that a high pressure environment significantly affects the penetration and evaporation rate of the spray.

The objective of this research is to investigate the cooling effect of the air jacket and air distributor in a spray dryer with a pressure nozzle. For the one forth of drum 3D model computation is used. The numerical model is based on a commercial computational fluid dynamics (CFD) package (Fluent). The simulated model and the computational results are compared with experimental measurement of a co-current spray dryer. For simulation, two different feeds are used: water and milk. RNG k-ε turbulent model, Euler-Lagrange models and SIMPLEC scheme are used to study the air path lines, temperature, humidity and velocity distribution of fluid, pressure field, wall temperature and particles temperature and humidity, time of evaporation and particle diameter. By tracking the particles through the flow domain their patterns are modelled and the exchange of mass, energy and momentum along the trajectories are calculated.

2. MATHEMATICAL MODEL

Based on the time average method for recirculation flow with isotropic turbulence perturbations and steady state conditions, the governing equations for quantities u, ρ, T can be written as:

$$u_{i,j} = 0 \tag{1}$$

$$\rho(u_j u_{i,j}) = -p_{,j} + [\mu(u_{i,j} + u_{j,i}) - \rho \overline{u_i' u_j'}]_j + \rho g_i \tag{2}$$

$$\rho C_p(u_j T_{,j}) = (k_1 T_{,j} - \rho C_p \overline{u_j' T'})_{,j} \tag{3}$$

Where u is velocity; i, j indicate differentiation index and $\overline{u_i' u_j'}$ denotes time average of a fluctuation quantity. For problems with rapid strain and streamline curvature flow separation, the RNG $k-\varepsilon$ turbulence model is more responsive than standard $k-\varepsilon$ model [11]. In this turbulent model the turbulence field is characterized in terms of turbulent kinetic energy (k) and the viscous dissipation rate of turbulent kinetic energy (ε). The k and ε equations of the RNG model can be written as:

$$\rho u_j k_{1,j} = [(\mu+\frac{\mu_t}{\sigma_k})k_{1,j})_{,j} + G_k + G_b - \rho\varepsilon \tag{4}$$

$$\rho u_j \varepsilon_{,j} = [(\mu+\frac{\mu_t}{\sigma_\varepsilon})\varepsilon_{,j}]_{,j} + C_1\frac{\varepsilon}{k}(G_k+C_3 G_b) - C_2\rho\frac{\varepsilon^2}{k} - R_\varepsilon \tag{5}$$

Where $\quad R_\varepsilon = \dfrac{C_\mu \rho \eta^3 (1-\frac{\eta}{\eta_0})}{1+\beta\eta^3}\dfrac{\varepsilon^2}{k} \quad , C_\mu = .0845 , \eta \equiv \dfrac{Sk}{\varepsilon} \; \eta_0 = 4.38 , \beta = .012 , C_1 = 1.42, C_2 = 1.68$

$$G_k = \mu_t S^2 \;, \; G_b = \beta g_i \frac{\mu_t}{\mathrm{Pr}_t}\frac{\partial T}{\partial x_i} \;, \; \beta = -\frac{1}{\rho}(\frac{\partial P}{\partial T})_p \;, \; C_{3\varepsilon} = \tan gh\left|\frac{v}{u}\right|$$

Where G_k is generation of turbulence kinetic energy due to the mean velocity gradients, G_b is generation of turbulence kinetic energy due to buoyancy, S_{ij} is rate of the mean strain tensor and μ and μ_t are coefficient of physical and turbulent viscosity respectively. Physical properties of air at 0.84 atmosphere (Shiraz pressure) and temperature between 250K to 450K with maximum error of 0.6 percent are calculated by:

$$\rho = 4.413 - .0207T + 4.263\times10^{-5}T^2 - 3.25\times10^{-8}T^3 \tag{6}$$

$$C_p = 945.94 + .624T - 2.203\times10^{-3}T^2 + 2.67\times10^{-6}T^{-6} \tag{7}$$

$$k = -0.016 + 2.556\times10^{-4}T - 5.397\times10^{-7}T^2 + 5.33\times10^{-10}T^3 \tag{8}$$

$$\mu = 2.41\times10^{-6} + 5.47\times10^{-8}T + 8^{-12}T^2 - 4\times10^{-14}T^3 \tag{9}$$

The spray dryer walls are made of AISI304 with 4mm thickness and its C_p is calculated by:

$$C_p = 63.9924 + 2.5092T - 4.7247\times10^{-3}T^2 + 3.2083\times10^{-6}T^3 \tag{10}$$

The particle motion, its trajectory, velocity, temperature and humidity are studied using the Euler-Lagrange method. The evaporating process and the final temperature of the particles is obtained by considering equations of heating droplets, evaporation and the mass transfer during the evaporating state [12]. Saffman's lift and thermophoretic forces are considered for particles [13, 14]. Also, the C_p of water droplet is calculated by:

$$C_p = 5.2058\times10^3 - 6.4956T + .0101T^2 + 5.0948\times10^{-7}T^3 \tag{11}$$

C_p of milk (specific heat at constant pressure) droplet is given by [15]:

$$C_p = 1.675 + .025\times(waterContent\%) \tag{12}$$

For milk, the initial density was considered and average thermal conductivity is determined by:

$$k_{milk} = (1-0.5X_{solid})k_{water} \tag{13}$$

Where X_{solid} is the percent of solid phase in the mixture. The droplets are evaporated at the wet bulb temperature of air [16], thus the wet bulb temperature is calculated as:

$$T_{wetBulb} = -118.3353 + 2.20901T - 2.9139 \times 10^{-3} T^2 \tag{14}$$

Where T is in degree Kelvin. One of the important parameters in spray condition is specifying saturated pressure. Incorrect pressure value will make a significant error in the solution. The saturated pressure is calculated as:

$$P_{sat} = 10933211.68 - 144519.32T + 720.752T^2 - 1.6084T^3 + 1.3595 \times 10^{-3} T^4 \tag{15}$$

In this study, the hollow cone pressure nozzle with 60 degree and 0.4 mm diameter is used. The nozzle is inserted 20 cm lower than the air distributor. The average diameter and velocity of droplets can be written as [17]:

$$u = v \tan \theta \, , \qquad v_{res} = (2g \frac{P}{\rho})^{\frac{1}{2}} \tag{16, 17}$$

$$D_{droplet} = 286(d_0 + 0.17)\exp(\frac{13}{v} - 0.0094u) \tag{18}$$

Where d_o is nozzle diameter. Equations (16) to (18) are empirical and properties are in English units (P (psi), ρ (lbm/ft³), velocity (ft/s), d_o (in) and Droplet (micron). By considering heat losses from the dryer walls and evaporation, the energy balance can be written as:

$$(\dot{m}C_p \Delta T)_{air} = (\dot{m}C_p \Delta T)_{water} + \dot{m}_{water} h_{fg} + Q_{Loss} \tag{19}$$

Regarding the above equation, a discharge of non-evaporated feed from a spray dryer can be obtained. After a few minutes from the beginning of the process, the system reaches steady state condition. The steady state simulation is carried out on the pilot plant spray dryer as shown in Figs. 1 and 2. Air enters the drying chamber in the axial flow direction from the air distributor plate with 0.125m diameter and 42 holes, each hole has a 2cm diameter. Cooling air, which exits from a blower fan, enters the secondary wall with helical passage, 0.5m pitch, around the drum in a counter-current direction with respect to the main process. A linear temperature for the cooling air is assumed therefore, it is found that;
1) Computational time decreased.
2) The calculated error between fluid outlet temperature obtained from software and experiments without spray was less than one percent.
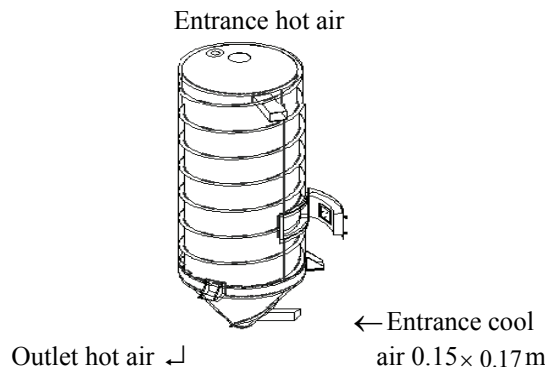

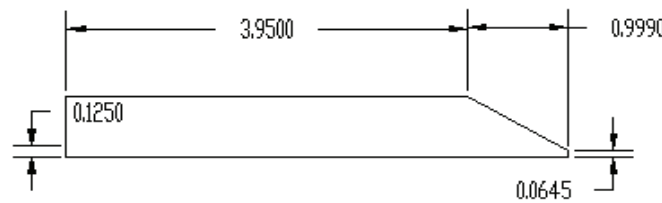Fig. 1. Schematic of spray dryer, 0.5m pitch, 1.308m inner diameter, 1.431m outer diameter

Fig. 2. A section of spray dryer, 2D model

It is assumed that air flows in a helical passage similar to the air flowing in a helical pipe. Mori and Nakayama [18] and Yang and Ebadian [19] proposed Nusselt number in a curved pipe as:

$$Nu = \frac{\text{Pr}}{26.2(\text{Pr}^{2/3} - .074)} \text{Re}^{0.8} (\frac{a}{R})^{0.1} (1 + \frac{0.098}{(\text{Re}(\frac{a}{R})^2)^{1/5}})$$ (20)

Where a is radius of the pipe and R is radius of curvature of the pipe axis. It is assumed that the average temperature in each pitch is constant. By considering a relation between bar external surface and heat transfer coefficient, the effective fin side heat transfer coefficient can be written as:

$$h_{fo} = \frac{h_f (\Omega_f A_f + A_u)}{A_b}$$ (21)

Where A_f is external finned surface per meter, A_u is external unffined surface per meter, A_b is bar external surface per meter, as though fins did not exist, h_{fo} is effective fin-side heat transfer coefficient, h_f is fin-side heat transfer coefficient and Ω_f is the fin efficiency. The fluid temperature and heat transfer coefficient profile are used for wall boundary conditions outside of the main chamber. For 3D model decrease mesh numbers, the study is made for one fourth of the drum, with the absence of a helical passage and a secondary wall. By considering 10% loss in pipes after passing along the flow line and by measuring the mass flow rate into the chamber, inlet air velocity is determined. A fully developed flow is considered for the inlet fluid from the air distributor. By multiplying average velocity by 1.05 for central holes, 1 for middle holes and 0.95 for side holes, inlet velocity for all holes are calculated. Table 1 shows the pressure loss in pipes from the outlet chamber of the spray dryer to the inlet of the cyclone and exerted pressure of fan on the outlet of the chamber from the cyclone fan. These values are approximately equal and modeling is relatively acceptable. It should be noted that zero gauge pressure is considered for the outlet boundary condition, and the velocity and temperature of the inlet fluid are considered for the inlet boundary condition. By simultaneous solution, convection heat transfer outside the chamber, heat conduction in the wall and free and forced convection within the chamber, temperature distribution in the chamber and its wall are determined.

Table 1. Comparison between measuring pressure of fan and
pressure loss in pipe based on Second Run

Pressure loss in pipe	829 (Pa)
Fan's measuring pressure	859.5 (Pa)

Evaporation of droplets occurs in two stages, first at a constant rate and second at a falling rate. In the first stage when the droplets contact hot air, the water evaporates at a constant rate. In the second period, the transfer of humidity from the droplets to the surface gradually decreases and decreasing humidity

causes a resistance against mass transfer. The required time for high temperature process is very short. The average rate of evaporation in the two stages (W and W') respectively are:

$$\frac{dW}{dt} = \frac{0.79 k_d D_{av} \Delta T}{h_{fg}} \tag{22}$$

$$\frac{dW'}{dt} = \frac{-0.05 k_d \Delta T}{h_{fg} D_c^2 \rho_s} \tag{23}$$

Where ΔT is given by:

$$\Delta T = \frac{\Delta T_0 - \Delta T_1}{4.19 \log_{10}(\frac{\Delta T_0}{\Delta T_1})} \tag{24}$$

The value of ΔT_0 and ΔT_1 are the first and second difference of temperature between the air and droplet during the evaporation process in each stage [17]. D_c is 60-80 percent of the first diameter, D_{av} is the average between the first and final diameter in each stage, ρ_s is density of solid and k_d is the coefficient of thermal conductivity of droplet. The necessary time required for evaporation can be obtained from adding the above equations. To validate the CFD model, the air temperatures were measured at the outlet of the process and cooling air. SIMPLEC and the second order upwind differencing schemes and the RNG k-ε method are used to relate pressure and velocity. A parallel solution with 6 computational nodes is used without spray, each node was 2400MB CPU and 1GB RAM. To check the grid independency, refined and coarse mesh are tested and the flow field and outlet temperature are calculated. Table 2 represents the comparison between the outlet temperature (without spray) and the experimental results. Therefore, 171350 cells are used without spray. Parallel solution needs shared memory with spray computation are carried in the high speed computational centre of Shiraz University with a distributed memory system. A personal computer with 2500MB CPU and 256 MB RAM is used for running the program in the spray solution. The results of 171350 and 142776 cells are close, therefore, the shorter running time (60 hours) with fewer cells are used.

Table 2. Mesh independent study for outlet temperature without spray,
second run, experimental temperature 381K

Grids $(r \times \theta \times y)$	Outlet temperature(K)	Runtime (Hr)
341582 ($52 \times 38 \times 178$)	376.1	16
171350 ($47 \times 28 \times 115$)	377.3	7.25
142776 ($44 \times 24 \times 108$)	377.2	4.25

3. MESH GENERATION

All cells near the walls are finer than other cells. The 'two layer' model or near wall model is used for the study of the flow near the wall. Also, for more accuracy, the cells near the inlet and outlet of the spray dryer in the axial flow direction and inlet flow of the chamber are generated finer than that of the inner cells. Figures 3 and 4 show an upper view of the model and outlet of the spray dryer.
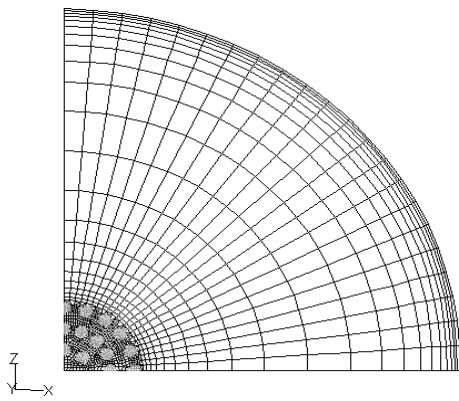
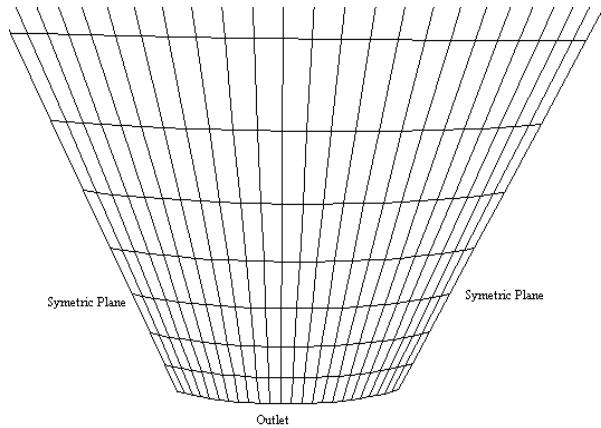Fig. 3. Upper views of model, circles are inlet flow

Fig. 4. Outlet of spray dryer

4. RESULTS AND DISCUSSION

Hot air enters from the air distributor, cold air enters in the cooling air jacket in the co-current direction, and feed enters from the nozzle that is inserted 20 cm lower than the center of the air distributor. For measuring air temperature, some thermocouples are inserted in the inlet and outlet of the cold and hot air flows respectively. Experiments are carried out in three runs, first and second with water spray and the third with milk spray. Discharge of feed at the first and second run is 0.0014 Kg/s and at the third run is 0.0016 Kg/s. By measuring air temperature and also calculating energy balance between hot and cold air, temperature and convection heat transfer coefficient for cooling air are determined, and the solution is based on trial and error. Table 3 shows a comparison between calculated energy losses (by convection and radiation from the first and second walls) and the difference between energy balances of hot and cold air which is obtained from software. There is an appropriate consistency between the software model and the experimental results. The calculation of the convection heat transfer coefficient in the cooling air (h) needs to determine the hydraulic diameter (D_h) and a/R in Eq. (20). In the cylindrical part of the drum, these two values can be determined easily, but in the cone part it requires special treatment. This part is divided in to four sections and each section was considered as a helical pipe. Effects of such variable hydraulic diameters and a/R causes a sharp variation of convection heat transfer coefficient in the entrance section of the cylindrical part. In the connected section between the cylinder and cone parts, the hydraulic diameter increases and causes the heat transfer coefficient to decrease. But in the cylindrical part, except for near the outlet, the hydraulic diameter decreases. Yet if the hydraulic diameter and a/R remain constant in this part, the thermal conductivity of air increases due to the increase of temperature. This effect causes the convection heat transfer coefficient to slightly increase. Figures 5-7 show D_h and a/R, temperature and convection heat transfer coefficient during the third run. Figure 6 shows that air enters with a low temperature and leaves with a higher temperature. Regarding the above figure, in the third run, air enters at a higher temperature than the first run. With spray milk, higher velocity, better mixing, and higher discharge causes flow outlet temperature to decrease. By using the nozzle diameter, the inlet flow from the pressure nozzle is divided in to the same number of tracking particles. By increasing the number of tracking particles the running time increases. Figure 8 shows the particle trajectory for different number of tracks and Table 4 denotes the total running time required for the solution with different tracking numbers. Table 5 shows inlet and outlet flow properties from computational and experimental data with and without spray. A good correlation is observed between experimental and computational results for the dryer without spray, but a significant difference is observed with spray. This difference is due to the slight difference in the computational simulation and experimental models. In this simulation, average particle

diameter causes the feed to convert to fine droplets, but for a real pressure nozzle fine and coarse diameters of droplets will be produced [17]. Therefore, large droplets will not evaporate completely and some particles will leave without complete evaporation. Table 6 shows discharge of evaporated and non evaporated feed from the spray dryer. Regarding Eq. (19), the amount of non evaporated discharge droplets causes the outlet temperature to decrease 5 degree in water spray and 2.6 degrees in milk spray. One of the important problems in the spray dryer is the amount of humidity in the system. After complete evaporation of water droplets, humidity near the wall is higher than in other parts. The particles near the wall enter in the opposite phase and absorb humidity from ambient [16, 17]. If the humidity exceeds the expected value, the particles will convert to clods. Fig. 9 shows radial relative humidity for milk spray at various sections. Near the wall at 0.5 m distance from the inlet, the temperature is lower and its humidity is higher than the other axial distance. Fig. 10 shows axial relative humidity; with decreasing temperature, humidity increases and vice versa. Figs. 11 and 12 show the axial velocity and temperature distribution. Adding spray causes sudden variations. At the entry, the velocity suddenly increases and the temperature drops suddenly. Then by mixing hot air and inlet spray, the velocity decreases and the temperature increases. Finally, heat loss and heat exchange cause the temperature to decrease. Free convection is caused by the high temperature difference between the wall and flow near the wall. Figures 13 and 14 show the comparison between the 2D path lines of the model for flows with and without free convection and without air distributor. With free convection, streamlines are different and for more accuracy free convection is also considered in the 3D model. Free convection causes positive velocity vectors to appear. Due to separation near the inlet, the reverse flow appears and the pressure is low. Positive velocity vectors decrease the power of the inverse flow and the flow inverse at lower axial distances. Figure 15 shows the axial pressure for both sprays. Based on the mass balance, the velocity in the outlet of the chamber increases and its pressure decreases. Figures 16 and 17 show the radial velocity distribution with and without milk spray. By increasing radial distance, velocity decreases. Feed enters into the spray dryer from the central holes and the air from around the holes of the air distributor. The velocity difference causes oscillation in the radial velocity distribution. By mixing the inlet flow, the oscillation of velocity disappears and velocity gradually increases. Radial temperature distribution with and without spray are shown in Figs. 18 and 19. By increasing radial distance, temperature decreases. Heat loss and heat exchange in the axial direction cause the temperature to decrease. Figures 20 and 21 show the centre line wall temperature with and without milk and water spray. Because of the high ratio of air to milk and water (200:1), the temperature with and without spray differ only 4-5 degrees. With spraying the milk, the main part of the wall is lower than 340K. Since the stickiness point of Lactose is 374K and the higher percentage of milk contains Lactose, regarding Table 7, a lower stickiness is observed. Figs. 22 and 23 show variation of temperature and humidity of 6 particles with respect to time. In order to obtain 50 lines tracking of particles, the first particle '1' and last particle '50' enter from the center and the edge of the simulated nozzle respectively. Other particle distribute between these two particles. When particles contact the wall, their temperature decrease suddenly. The temperature of the particles near the wall and also the temperature of last particles from the spray dryer are approximately 340K. Humidity distribution is changed opposite to the temperature distribution. Considering these figures and Fig. 8, the particles near the center line have more time and place for tracking and this causes the particles with few numbers to stop less than the particles with higher numbers. Figure 24 shows particle diameter variation with respect to time. This figure illustrates that the time of evaporation is about 0.02 s. Table 8 shows the time of evaporation which is obtained from the solution of Eqs. (22) and (23). This table shows that the total time of evaporation is 0.018 s. Crosby and Marshall's graphical method is also used to approximate initial

particle diameter. Fig. 25 shows the graphical calculation of the diameter distribution of particles. The average initial diameter of particles (which is used in the software) is 31 microns and the calculated diameter of the particles from figure 25 is 15.3 microns. By using a graphical method, Fig. 25, the final diameter is obtained as 16 microns. These results show that there is a good agreement between the software and the obtained results from empirical relations for the time of evaporation and particle diameters. Creating uniform distribution of temperature and particles are two important reasons for using an air distributor. The comparison between these obtained results and the 2D numerical model (without air distributor) indicates that there is uniform air distribution in the spray dryer.

Table 3. Comparison between calculated energy losses of numerical and experimental results

Run Number	Hot air (1) (numerical)	Cold air (2) (numerical)	Free convection and radiation (calculated from experimental result)	Difference, (1)-(2)
First	10707.2	8277.8	2050.2	2129.4
Second	11191.4	9146	1814.5	2045.4
Third	13296	12084.7	1033.2	1211.3
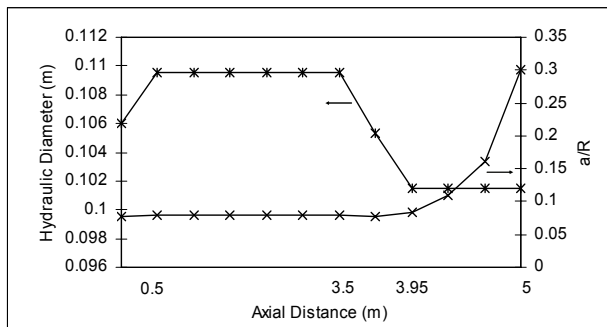
Fig. 5. Variations of D_h and a/R along axial distance
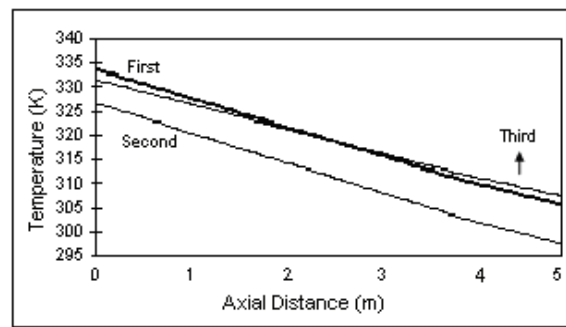
Fig. 6. Cooling air temperature distribution along axial distance
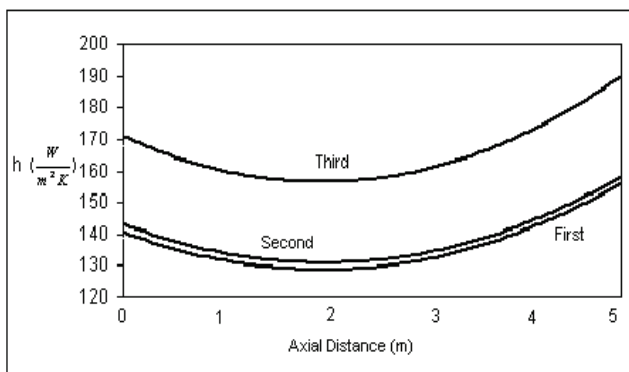
Fig. 7. Convection heat transfer distribution for three runs
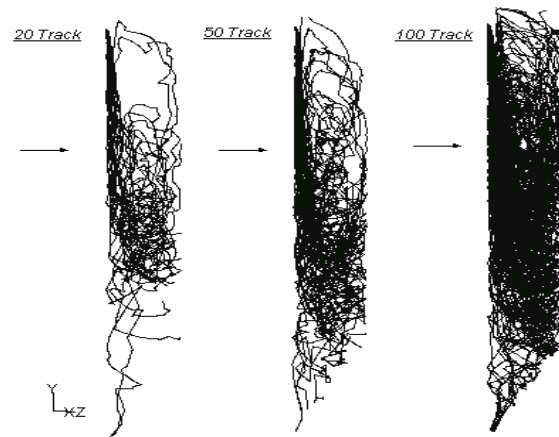
Fig. 8. Trajectories of particles with different tracking number

Table 4. Total running time required with different tracking number (Hr)

Number of tracking	Air	Discrete phase model	Total
20	31	12	43
50	31	29	60
100	31	58	89

M. Mohammadi et al.

Table 5. Inlet and outlet hot air and feed temperature, discharge of hot air and feed

Run number	Inlet hot air(K)	Outlet, hot air, without spray, software (K)	Outlet, hot air, wth spray, software (K)	Outlet, hot air, without spray, experimental (K)	Outlet, hot air with spray, experimental (K)	Feed (K)	Inlet cold air (K)	Discharge hot air-cold air (Kg/s)	Pressure-velocity of feed (Kg/s-m/s)
First	427	379.8	360	383	373	291.6	307	0.23 -0.31	10 - 40.8
Second	427	377.2	358.7	381	371	291	299	0.24 -0.30	10 - 40.8
Third	437	384.8	364.4	379	365	298	308.7	0.23 -0.50	30 - 64.5

Table 6. Discharge of evaporated and non evaporated
feed (exhaust water)

Run Number	$\dot{m}_{vapor}(\frac{kg}{s})$	$\dot{m}_{Exhaust-water}(\frac{kg}{s})$
First	8.7×10^{-4}	5.1×10^{-4}
Second	9×10^{-4}	4.8×10^{-4}
Third	1.4×10^{-4}	2.5×10^{-4}
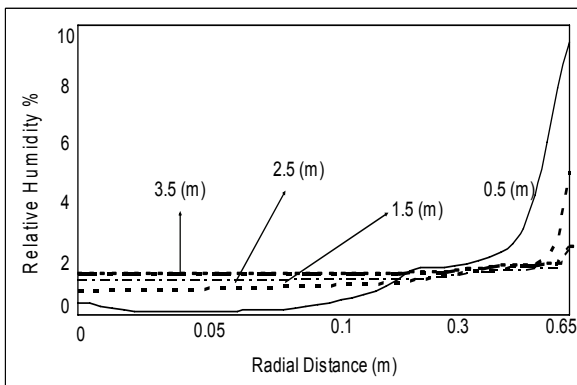
Fig. 9. Radial relative humidity along axial distance at different sections
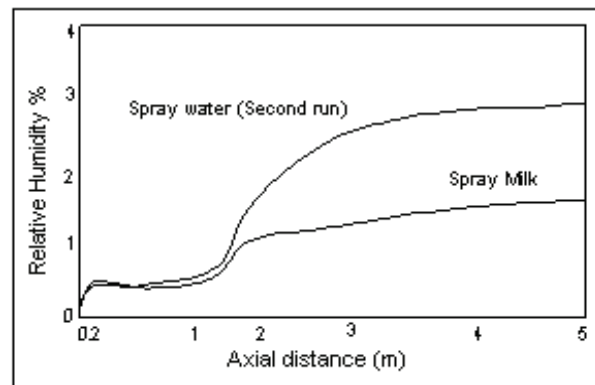
Fig. 10 Axial relative humidity variation for water and milk spray
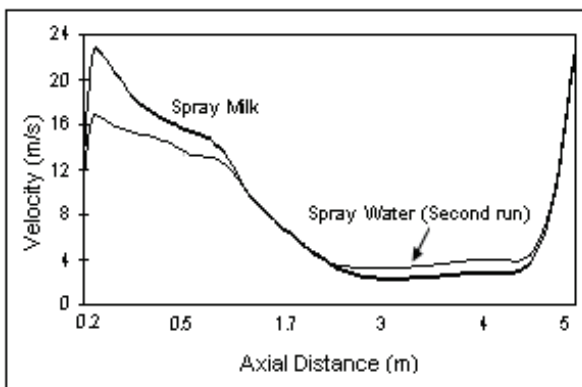
Fig. 11. Axial velocity distribution for water and milk spray
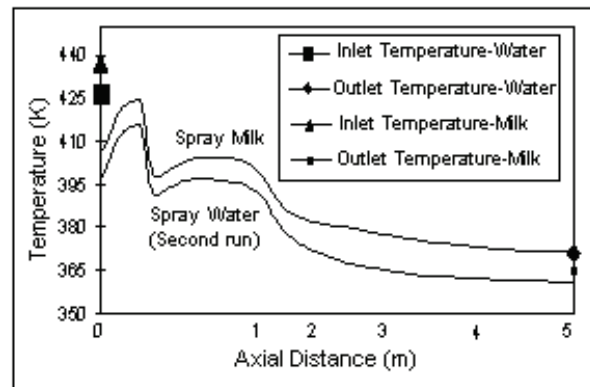
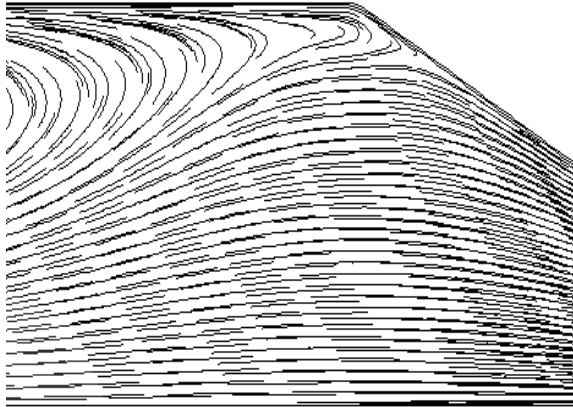Fig. 12. Axial temperature distribution for water and milk spray

Fig. 13. Flow path lines without free
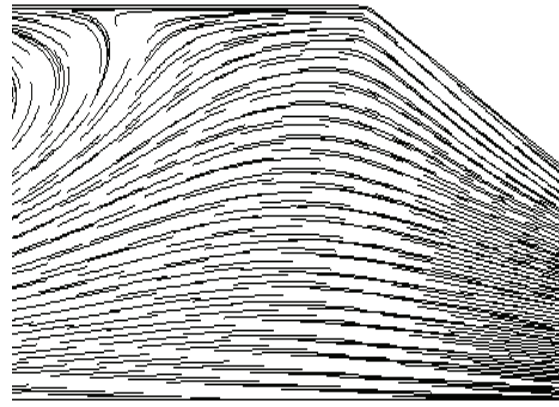convection, 2D model

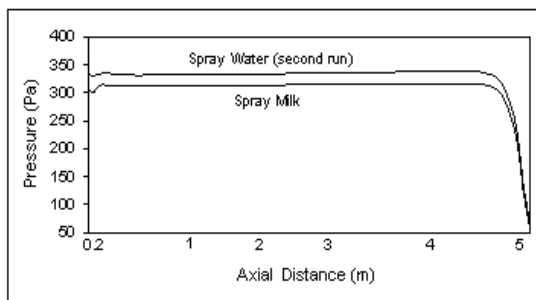Fig. 14. Flow path lines with free convection, 2D model

Fig. 15. Axial pressure distribution for
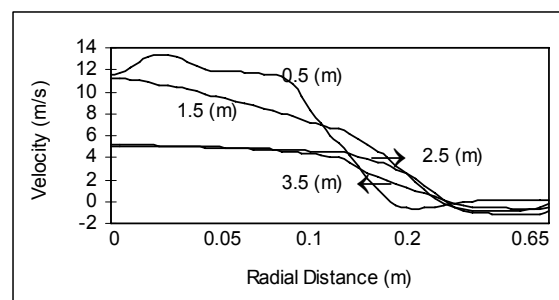water and milk spray

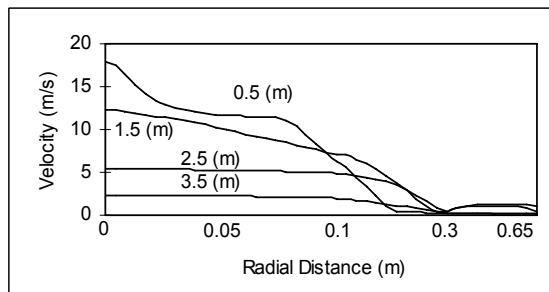Fig. 16. Radial velocity distribution without
spray at various sections

Fig. 17. Radial velocity distribution with spray milk at
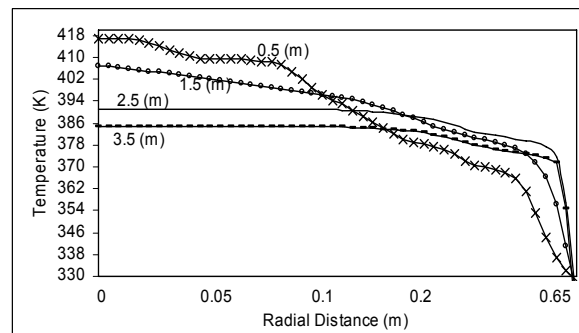various sections

Fig. 18. Radial temperature distribution without spray
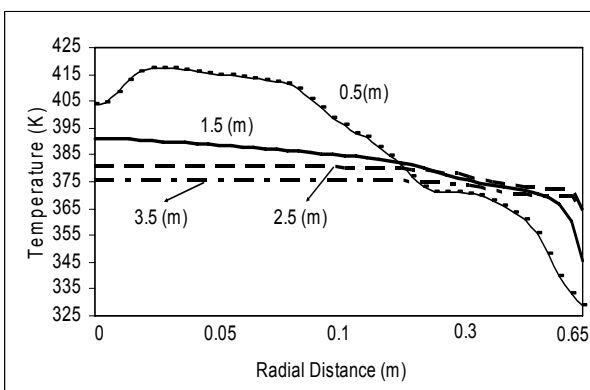milk at various sections

Fig. 19. Radial temperature distribution with spray
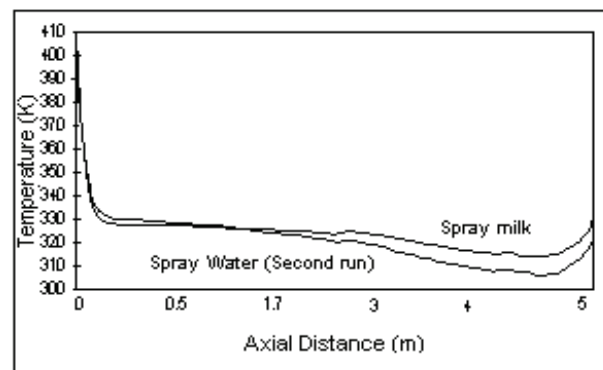milk (K) various sections

Fig. 20. Calculated inside centre line wall temperature
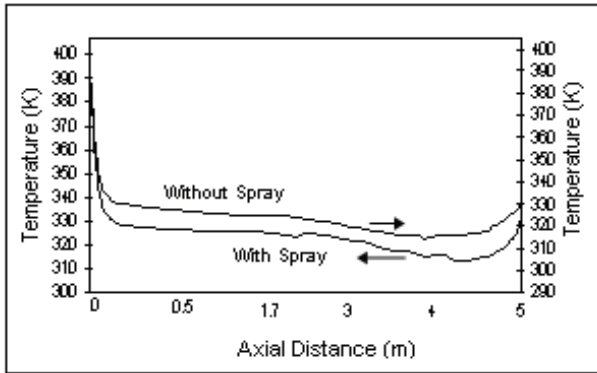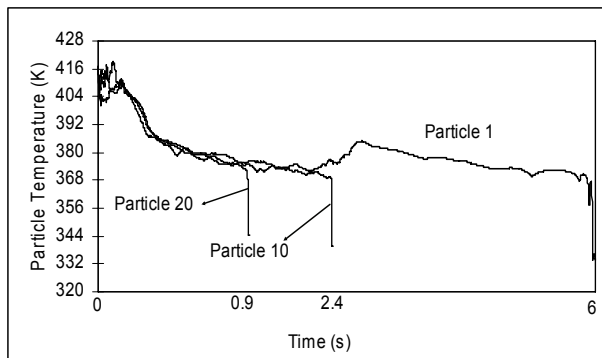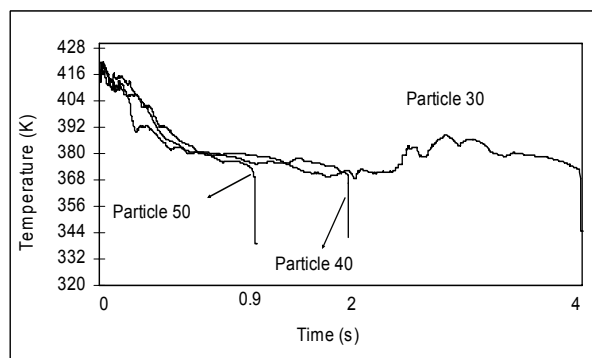of drum with spray milk and water

M. Mohammadi et al.

Fig. 21. Calculated inside centre line wall temperature
of drum with spray milk

Table 7. Stickiness point for sugars

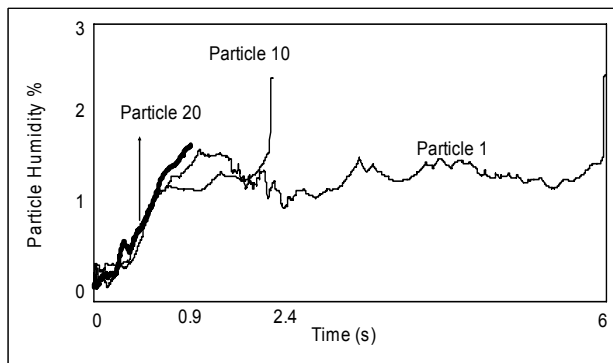| Sugars	Temperature (K)
Lactose	374
Maltose	360
Sucrose	335
Glucose	304
Fructose	278

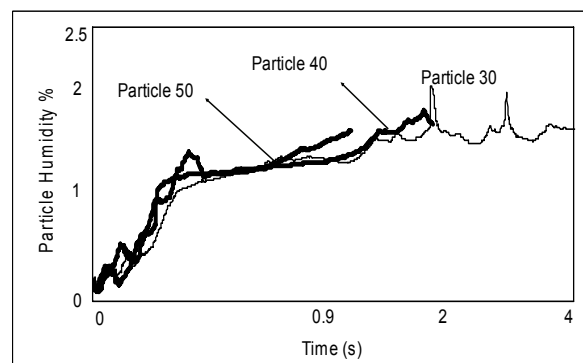a) Particles with low numbers

b) Particles with high numbers

Fig. 22. Variation of particle temperature with time

a) Particles with low numbers

b) Particles with low numbers
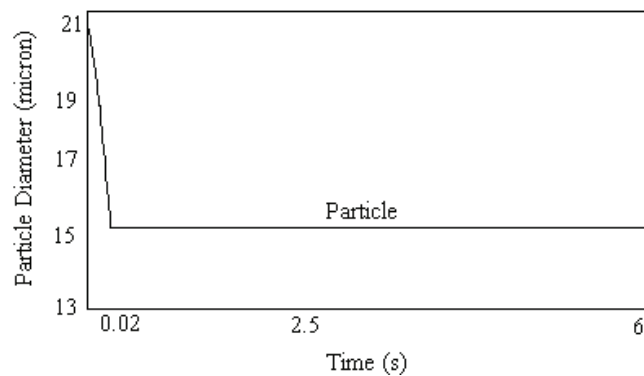
Fig. 23. Variation of particle humidity with time

Fig. 24. Variation of particle diameter contains spray milk with time

Table 8. Constant rate and falling rate time of evaporation

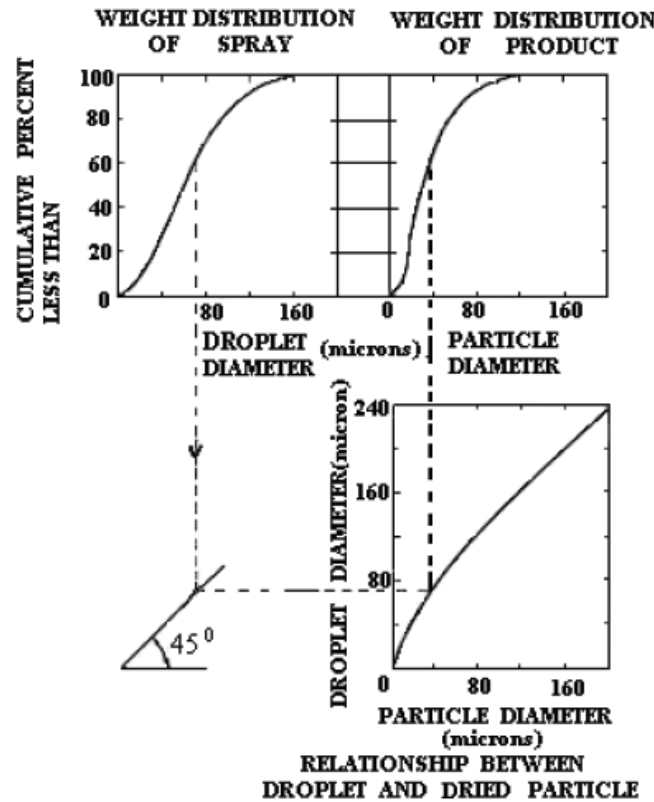| Material	Constant rate (s)	Falling rate (s)
Milk	2.1×10^{-3}	0.016

Fig. 25. Graphical method for approximation calculation of particle diameter

5. CONCLUSION

The objective of this article was to investigate the cooling air jacket and air distributor effects in a spray dryer with pressure nozzle. The modeling study and validation measurements are carried for a co-current spray dryer. According to the results:

1) Without spray, there is a high correlation between the present model and the experimental results.

2) By using average diameter for particles in the computational model, and comparing to the experimental measurement; with spray; the droplet did not evaporate completely, some differences between the software and experimental results are observed.

3) Using a cooling air jacket is useful to decrease the wall temperature for important sugars like Lactose, Maltose and Sucrose that are present in milk and fruit juices. Taking into account the high ratio of milk containing Lactose, the distribution of wall temperature indicates that there is low stickiness on most parts of the dryer wall.

4) Flow separation creates low pressure behind the main flow which results in an inverse flow due to the wall.

5) High difference of temperature between wall and flow near the wall causes free convection and positive velocity vectors.

6) Without using the air distributor, the comparison between the two cases with and without free convection for the 2D model, show some differences between the path lines, therefore free convection should be considered in 3D modeling.

7) Positive velocity vector due to free convection causes the power of inverse flow near the wall to decrease and flow reverse at the lower axial distance.

8) Air distributor causes velocity and temperature oscillation in both axial and radial distribution. But by increasing the axial distance, the effect of the air distributor decreases and the oscillation disappeared.

9) High correspondence is observed for time of evaporation and particle diameter from software with empirical relations .

10) Comparison of numerical results with the 2D model (without air distributor) indicate that there is uniform air distribution in the spray dryer.

NOMENCLATURE

a	radius of the pipe	k	coefficient of thermal conductivity
A_b	bar external surface per meter, as though fins did not exist	k_1	kinetic energy
A_f	external finned surface per meter	k_d	coefficient of thermal conductivity of droplet
A_u	external unfined surface per meter	p	Pressure
C_D	drag coefficient	R	radius of curvature of the pipe axis
C_p	specific heat at constant pressure	S_{ij}	rate of the mean strain tensor
D_{av}	average diameter of droplet	T	Temperature
D_c	critical diameter of droplet	u	velocity
d_o	nozzle diameter	X_{solid}	percent of solid phase
G_k	generation of turbulence kinetic energy due to the mean velocity gradients	ε	turbulent dissipation rate
G_b	generation of turbulence kinetic energy due to buoyancy	μ	coefficient of viscosity
g	Gravity	ρ	density
h_f	fin-side heat transfer coefficient	ρ_s	is density of solid
h_{fg}	latent heat	Ω_f	fin efficiency
h_{fo}	effective fin-side heat transfer coefficient		

Subscript   ***Superscript***

,	denotes derivative	'	denotes fluctuation in turbulent flow, conventionally averaged variable
i, j	grid locations in x, y, z directions	-	denotes average quantity of time average quantity
D	droplet		
S	solid		
t	turbulent		

REFERENCES

1. Bhandari, B. R., Dalta, N. & Howes, T. (1997). Problems associated with drying of sugar-rich foods. *J. Drying Technology,* Vol. 15, No. 2, pp. 671-684.

2. Bhandari, B., Dalta, N., Crooks, R., Howes, T. and Rigby, S. (1997). A semi-empirical approach to optimize the quantity of drying aids required to spray dry sugar-rich foods. *J. Drying Technology*, Vol. 15, No. 10, pp. 2509-2525.

3. Bhandari, B., Senoussi, A., Dumoulin, E. D. & Lebert, A. (1993). Spray drying of concentrated fruit juices. *J. Drying Technology*, Vol. 11, No. 5, pp. 1081-1092.

4. Oakley, D. E. & Bahu, R. E. (1991). Spray/gas mixing behavior within spray dryer. *J. Drying*, pp. 303-313.

5. Zbicinski, I. (1995). Development and experimental verification of momentum. Heat and mass transfer model in spray drying, *J. The Chemical Engineering*, Vol. 58, pp. 123-133.

6. Straastma, J., Houlingen, G. V., Streenbergen, A. E. & Jong, P. D. (1991). Spray drying of food products:1. Simulation model. *J. Food Engineering*, Vol. 42, pp.67-72.

7. Kieviet, F. G. (1997). Modeling quality in spray drying. Thesis, Eindhoven University of Technology, Eindhoven.

8. Aziztaemeh, H., Kazemi, A. A. & Razavi, J. (2005). Pomegranate juice powder production. *IJFST*, Vol. 2, No. 3.

9. Chegini, G. R. & Ghobadian, B. G. (2007). Spray dryer parameters for fruit juice drying. *World Journal of Agricultural Sciences*, Vol. 3, No. 2, pp. 230-236.

10. Khaleghi, H., Ganji, D. D. & Omidvar, A. (2008). Comparison of various droplet break up models in gas liquid flows in high pressure environment. *Iranian Journal of Science and Technology, Transaction B, Engineering*, Vol. 32, pp. 385-400, 2008.

11. Shaeri, M. R. & Yaghoubi, M. (2009). Numerical analysis of turbulent convection heat transfer from an array of perforated fins. *International Journal of Heat and Fluid Flow*, Vol. 33, pp. 218-228.

12. Manual of Fluent. INC.

13. Ranz, W. E. & Marshall, W. K. (1952). Evaporation from Drops: Part I. *J. Chem. Eng. Progress*, Vol. 48, No. 3, pp. 141-146.

14. Ranz, W. E. & Marshall, W. K. (1952). Evaporation from Drops: Part II. *J. Chem. Eng. Progress*, Vol. 49, No 4, pp.173-180.

15. Heldman, D. & Sing, P. (1990). Food industry engineering.

16. Sino, Y. & Keey, R. B. (1981). The drying of spherical particle containing colloidal material into a hollow sphere. *J. Chemical Engineering Science*, Vol. 37, No. 6, pp. 881-889.

17. Masters, K. (1976). *Spray drying*. 2nd. Ed, John Wiley & Sons, New York.

18. Mori, Y. & Nakayama, W. (1967). Study on forced convection heat transfer in curved pipes. *J. Heat Mass Transfer*, Vol. 10, pp. 37-59.

19. Yang, G. & Ebadian, M. A. (1996). Turbulent forced convection in a helical pipe with substantial pitch. *J. Heat Mass Transfer*, Vol. 39, pp. 2015-2022.

20. Saunders, E. A. D. (1988). *Heat exchangers*. John Wiley & Sons, New York.

21. Tannehill, J. C., Anderson D. A. & Pletcher, R. H. (1997). *Computational fluid mechanics and heat transfer*. Taylor & Francis, Philadelphia.